# 3D Microprobe Analysis of Dendritic Structures in Steel

J. Domitner
Christian Doppler Laboratory for Multiphase Modeling of Metallurgical Processes, University of Leoben, Austria

A. Kharicha, A. Ludwig, M. Grasser
Chair of Simulation and Modeling of Metallurgical Processes, University of Leoben, Austria

Keywords: 3D-reconstruction, dendritic structures, microprobe, microsegregation

## Abstract

In this paper, a novel method is presented which enables the reconstruction of three-dimensional dendritic structures by using concentration maps of a certain alloying element. For this purpose, a sample of conventionally produced continuous casting steel has been investigated. The determination of the two-dimensional maps has been performed at an electron probe microanalyzer (EPMA or "microprobe") equipped with wavelength dispersive spectrometers (WDS). After the EPMA measurements, a commercial software tool has been utilized to process the concentration maps into three-dimensional structures. The dendritic structures created by this method can be used for further investigations in FEM- or CFD-simulation tools.

## Introduction

In the field of numerical simulations, such as computational fluid dynamics (CFD) or structural mechanics for example, the geometric representation of the investigated structures is an essential input parameter to perform a simulation. If a certain structure has a well defined geometrical shape, it is comparatively easy to create its representation by using miscellaneous computer aided design (CAD) tools. In most cases in technical engineering this may apply, but naturally growing structures have a quite complex shape and therefore they can not be described with simple geometric relations. A common way to make such structures also available for numerical simulations is to detect their shape using different measurement techniques and to import the generated geometric information into the simulation software afterwards.

For instance in advanced metallurgy, the computed tomography (CT) [1] or the serial sectioning method [2, 3] are often used to visualize three-dimensional dendritic structures. Both of these methods deliver only the geometric representation of the dendrites at a certain stage of solidification, but the varying dendritic shape during progressive solidification is not captured. Especially for a detailed investigation of solidification processes this is deficient, because most parameters to describe a dendritic structure (e.g. such as permeability, solid-liquid interface, volume fraction of solid, …) strongly change with the evolution of the dendrites. To capture their changing shape during solidification, comparatively elaborate in situ observations (e.g. the high-speed X-ray microtomography [4]) are required. Nevertheless, it would be more convenient to get an appropriate estimation of the dendritic growth by investigating a completely solidified sample at room temperature. Therefore the quantity to be measured must correlate more or less

with the evolving dendritic shape during the previous solidification process. For example, the concentration of a certain alloying element inside the solidified metal represents such a "growth-dependent" quantity.

In steel, the solubility for most alloying elements of practical use is higher inside the melt than inside the forming solid. These elements are rejected from the solid during the solidification process, whereas their content inside the liquid phase increases continuously. Thus, the first forming solid contains a lower content of alloying elements than the solid forming out of the highly enriched melt at the end of solidification [5]. This segregation tendency at microscale level is utilized for the reconstruction method presented in the current paper. After gathering several concentration patterns for the alloying element manganese from a completely solidified sample, all measured values having the same concentrations were connected with surfaces. These iso-concentration surfaces represent the dendritic structure at a certain stage of solidification. Hence, it is possible to visualize the dendrites and to provide the determined geometrical data for further simulation work afterwards.

## Reconstruction Procedure

A schematic overview of the reconstruction procedure presented in this paper, covering sample preparation, microprobe measurements and concentration map processing, is given in Fig. 1. Notice, that the steps b) - d) were performed five times.

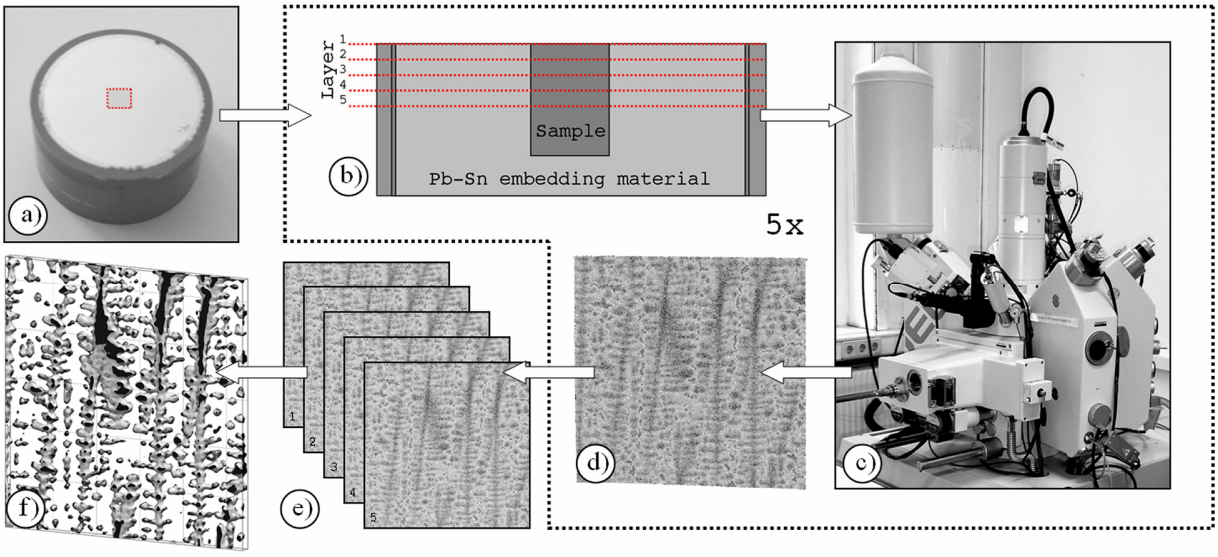


*Figure 1: Schematic overview of the presented reconstruction procedure; a) sample taking and embedding, b) preparing the sample for the measurement (removing a defined layer thickness and surface polishing), c) microprobe measurement with WDS, d) concentration map processing, e) map alignment, f) reconstruction of the dendritic structure.*

## Sample Preparation

During the continuous casting process of steel, the surface of the slab is cooled rapidly with water. That causes a steep temperature gradient along the slab's thickness. Therefore, a fine microstructure as well as an oriented growth of columnar dendrites from the surface to the center

occurs. Cropping a sample parallel to this growth direction beneath the slab's surface ensures that the entire dendrites and not only fragmented parts of them remain inside the sample. For this reason the investigated sample, having a cross section area of approximately 3 x 3 mm in square, was taken 35 mm below the surface and parallel to the dendritic growth direction.

To prepare this sample for the following microprobe measurements, it was embedded into a low melting eutectic alloy, composed of tin and bismuth [6]. On the one hand, this embedding material ensures the required conductivity of electricity between the sample holder inside the microprobe and the sample itself. On the other hand, the material is resistant against the electron beam of the microprobe, which allows the measurement in the embedding area surrounding the investigated sample, too. The considerable difference in the measured manganese concentration between the sample and the embedding material can be used to detect the sample's boundaries and to align each concentration map along these boundaries afterwards.

Clean and well polished sample surfaces are an essential precondition to get accurate microprobe analysis results. To achieve this, the investigated steel sample was first polished with a mono-crystalline 3 µm diamond suspension on a satin woven natural silk cloth, which affords fast material removal. Then, the final polishing to finish the sample's surface was accomplished with a mono-crystalline 1 µm diamond suspension on a porous neoprene cloth. For these two polishing steps, a semi-automated polishing machine was utilized. Following this procedure, a material layer of 25 µm (± 3 µm) thickness was removed after each microprobe measurement, checked by control surveys with a digital indicating calliper. It has to be mentioned that microprobes equipped with focussed ion beams (FIB) allow an immediate material removal directly inside the sample chamber during the measurement procedure [7]. Nevertheless, this is only efficient for investigated areas of few microns and therefore not applicable in the current case with an area of more than 3 x 3 mm.

## Microprobe Measurements

The reconstruction method presented in this paper is based on a set of five concentration maps, measured with wavelength dispersive spectrometers (WDS) at a JEOL 8200 electron probe microanalyzer (EPMA, microprobe). Each of these maps, taken from different depths of the investigated steel sample, consists of 660 x 660 pixels and each pixel represents a measured concentration value of manganese on a pretty small square area of 5 x 5 µm. The main conditions and basic settings for the performed measurements are listed in Tab. 1 below.

**Table 1: Conditions and basic settings for the microprobe measurements**

| | |
|---|---|
| Analyzed element: | Manganese (Mn) |
| Analyzing crystal: | Lithium fluoride (LIFH) crystal |
| Acceleration voltage: | 15 kV |
| Electron beam current: | 250 nA |
| Preset value for the probe diameter: | 0 µm (focussed) |
| Dwell time per measurement point: | 120 ms |
| Interval between measured points: | 5 µm (in horizontal x- and y-direction) |
| Number of measured points: | 660 x 660 |
| Investigated total area per map: | 3300 x 3300 µm |
| Required measurement time per map: | ~ 16 hours |

Fig. 2 shows one of the original concentration maps, measured at the JEOL 8200 microprobe. The different levels of gray represent the detected concentration distribution of manganese at the investigated sample surface. The black frame surrounding this grayscale map is due to the extremely low manganese content of the embedding material. This difference in concentration allows the detection of the map boundaries and therefore an exact alignment of each map along these boundaries.

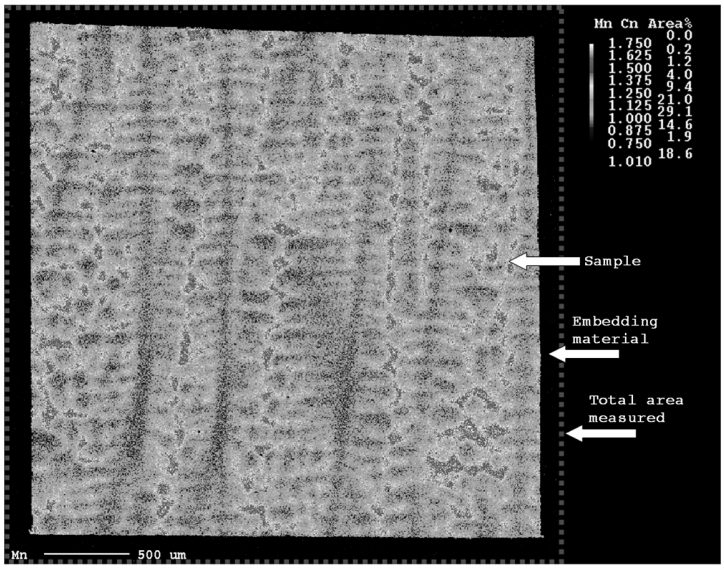


*Figure 2: Typical measured concentration map for manganese*

## Concentration Map Processing

The maps created at the microprobe comprise thousands of pixels with the corresponding concentration values. It is typical for the utilized microprobe mapping method that no smooth concentration transitions between adjacent pixels occur. Thus, connecting the concentration values directly after the measurement would create cragged instead of smooth surfaces. Hence, a preliminary smoothing of each concentration map was necessary, which was performed in two steps utilizing the software package MATLAB®.

First, undesired peak values of concentration were removed from the measured maps. For instance, minute holes, non-metallic inclusions or impurities (such as dust particles) on the sample's surface may cause concentration peaks, if the electron beam passes them during the measurement. Since such peaks are not immediately connected with the occurring segregations during the growth of the dendritic structure, it is necessary to remove them from the measured maps. For this purpose a median filter, expressed by Eq. 1, was utilized [8]. In a second step, a Gaussian filter was applied to the median filtered maps to achieve smooth concentration transitions required for the reconstruction. The Gaussian filter is defined by Eq. 2 afterwards [9].

$$C_{S'}(x,y) = \underset{(i,j)\in R_{x,y}}{\text{median}} \{C_S(x+i, y+j)\} \qquad (1)$$

$$C_{S''}(x,y) = \sum_{(i,j)\in R_{x,y}} C_{S'}(x+i, y+j) \cdot \mathrm{e}^{-\frac{i^2+j^2}{2\sigma^2}} \qquad (2)$$

In the previously mentioned equations, $C_S$ represents the concentration of a certain pixel measured with the microprobe. $C_{S'}$ stands for the concentration after applying the median filter and $C_{S''}$ is the final concentration after applying the Gaussian filter. The local filter coordinates $i$ and $j$ are only valid inside the filter area $R_{x,y}$ which surrounds a certain pixel at the global Cartesian map coordinates $x$ and $y$. The chosen parameters for both of these filter types are summarized in Tab. 2.

**Table 2: Map processing parameters**

| | |
|---|---|
| Size of the median filter area: | 9 x 9 pixels |
| Size of the Gaussian filter area: | 9 x 9 pixels |
| Gaussian filter width $c$ : | 2 pixels |

## Map Alignment and 3D-Reconstruction

The smoothed maps were stored inside a three-dimensional matrix, one single map per matrix layer. Before, the outer frame of each map was cut off to ensure, that only concentration values from the sample itself and not from the surrounding embedding material were stored. The final concentration matrix and therefore the structure created from the matrix data have an overall size of 550 x 550 x 5 pixels or 2750 x 2750 x 100 µm, respectively. Additionally, mathematical operations to consider the influence of curvature and temperature gradients on the concentration field can be applied at this stage of the reconstruction process. More details about the curvature calculation based on the measured and smoothed concentration maps can be found in reference [10].

Finally, the reconstruction of the dendritic structure was achieved by connecting all matrix entries having the same predefined concentration value of manganese with surfaces. These surfaces represent the shape of the dendrites at a certain stage of solidification. In the following, the growth of the dendritic structure depending on three ascending iso-concentration values is shown. Exporting these structures (e.g. using *.stl or *.wrl file formats) makes them available for further processing in computer aided design or numerical simulation tools, preconditioned that sufficient computational power is available.

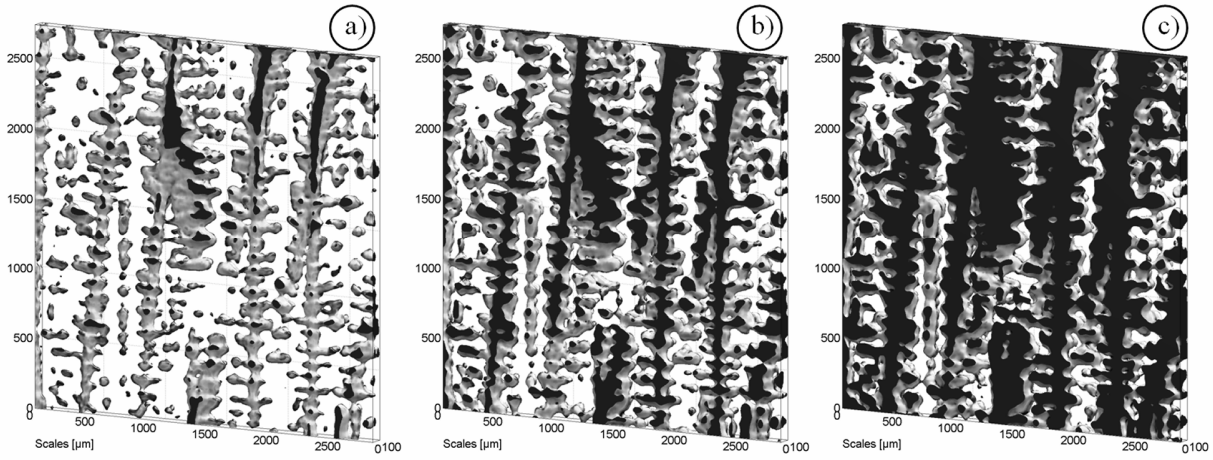


*Figure 3: Different fractions of solid depending on the predefined concentration values of manganese; a) 1.00 % Mn, b) 1.05 % Mn, c) 1.10 % Mn*

## Structure Evaluation

### Segregation Tendency of Manganese

To characterize the microsegregation tendency of manganese during solidification, the concentration $C_S^{\mathrm{Mn}}$ at the surface of the created dendrites was correlated with the dendrite's volume. As shown in Fig. 4 below, $C_S^{\mathrm{Mn}}$ increases with advancing solidification and therefore with rising solid fraction $f_S$. It has to be mentioned that for low solid fraction ($f_S < 0.1$) the plotted curve gives only an approximation of the actually appearing concentrations. At such low volume fractions special growth phenomena (e.g. concentration enrichment in front of the thin dendrite tips) may occur, which are not considered in the current reconstruction model. The dashed horizontal line in Fig. 4 shows the average manganese concentration $C_0^{\mathrm{Mn}}$ inside the investigated sample.

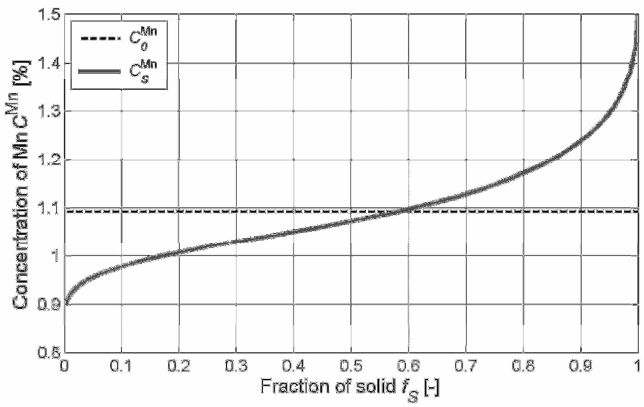


*Figure 4: Mn-concentration at the dendrite's surface depending on the solid fraction*

### Solid-Liquid Interface Area

To describe the evolution of the dendritic surface area $A_{SL}$ which represents the solid-liquid interface between the melt and the forming dendrites, the area-volume ratios $S_{V,T}$ and $S_{V,S}$ are introduced. Notice that the reconstruction of the dendritic structure presented here is based on the investigation of a totally solidified sample. Therefore, "liquid" means the solid sample domain containing larger and "solid" the sample domain containing lower concentration values than the pre-defined value to visualize the dendritic surface. $S_{V,T}$ and $S_{V,S}$ are defined as shown in Eq. 3 and Eq. 4 below. For these ratios, $A_{SL}$ is related to the total sample volume $V_T$ or only to the volume of the developing solid $V_S$, respectively.

$$S_{V,T} = \frac{A_{SL}}{V_T} \quad (3)$$

$$S_{V,S} = \frac{A_{SL}}{V_S} \quad (4)$$

Depending on the solid fraction $f_S$, the curves for these ratios are illustrated in Fig. 5 afterwards. It is apparent that $S_{V,T}$ has a maximum value at $f_S \approx 0.4$, whereas it becomes zero at $f_S = 0.0$ and $f_S = 1.0$. However, with advancing solidification $S_{V,S}$ decreases rapidly towards zero.

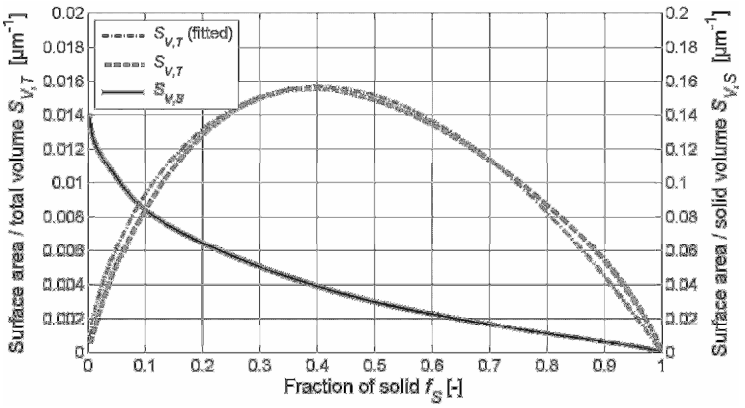


*Figure 5: Solid-liquid interface area ratios depending on the solid fraction*

One can approximate the depicted curve for $S_{V,T}$ with the generally-known relationship

$$S_{V,T} = C \cdot {f_S}^a \cdot (1 - f_S)^b, \quad (5)$$

wherein the empirical constant $C$ as well as the exponents $a$ and $b$ are chosen to fit the experimental data. Several proposals can be found for $a$ and $b$ in literature, such as $a = b = 1$ (Speich and Fisher [11]), $a = b = 2/3$ (Cahn [12]) or $a = 0.517$, $b = 0.467$ (Limodin et al. [4] according to Rath [13]). Furthermore, Ratke and Genau derived an analytical model to describe the evolution of the specific surface area during solidification using $a = 1/2$ and $0 < b < 1$ [14]. As shown in Fig. 5 above, it is possible to fit the curve for $S_{V,T}$ with $C = 0.048\,\mu\text{m}^{-1}$, $a = 2/3$ and $b = 1$. Nevertheless, it has to be mentioned that the effect of an occurring temperature gradient on the investigated microsegregation pattern and therefore on the dendrite's shape and on the curves of Fig. 5 is neglected. Considering this gradient is an ongoing work.

## Conclusions

Providing accurate model geometries close to reality is one of the basic requirements to perform direct numerical simulations in modern engineering sciences. For this reason, the method presented in this paper offers a possibility to reconstruct three-dimensional dendritic structures in metals to use them for further investigations in FEM- or CFD-simulations. The reconstruction method is based on several concentration maps of a certain alloying element, measured with wavelength dispersive spectrometers at a microprobe. In steel, it is beneficial to focus on the concentration distribution of manganese, due to its distinct microsegregation tendency. Since the concentration maps must be taken from different depths, the serial sectioning of the investigated sample is required between each microprobe measurement. To prepare them for further processing, the measured concentration patterns are smoothed with different image filters. Afterwards, the concentration maps are stored in a three-dimensional matrix, one single map per matrix layer. Then all matrix entries having the same predefined concentration value are

connected with surfaces. Since the alloying element concentration increases during advancing solidification, these iso-concentration surfaces represent the shape of the dendrites at a certain solidification stage. Finally, a simple correlation was used to relate the specific surface area with the solid fraction.

## Acknowledgments

The authors would like to thank the industrial project partners Materials Center Leoben Forschung GmbH (MCL), voestalpine Stahl GmbH, voestalpine Stahl Donawitz GmbH & Co KG and Siemens VAI Metals Technologies GmbH & Co for their contributions to this project. Thanks go to Mrs. Judith Fluch from voestalpine Stahl GmbH as well as to Mrs. Federica Zaccarini and Mr. Helmut Mühlhans from the University of Leoben for supporting the microprobe measurements. Special thanks go to Mr. Siegfried Schider from the Materials Center Leoben Forschung GmbH for the excellent preparation of the investigated sample.

## References

[1] D. Fuloria, P. D. Lee, and D. Bernard, Microtomographic characterization of columnar Al-Cu dendrites for fluid flow and flow stress determination, *Mater. Sci. Eng. A*, Vol 494, 2008, p 3-9

[2] J. Alkemper, and P. W. Voorhees, Quantitative serial sectioning analysis, *J. Microsc.*, Vol 201, 2001, p 388-394

[3] J. Madison, J. E. Spowart, D. J. Rowenhorst, and T. M. Pollock, The Three-Dimensional Reconstruction of the Dendritic Structure at the Solid-Liquid Interface of a Ni-Based Single Crystal, *JOM*, Vol 60 (No 7), 2008, p 26-30

[4] N. Limodin, L. Salvo, E. Boller, M. Suéry, M. Felberbaum, S. Gailliègue, and K. Madi, In situ and real-time 3-D microtomography investigation of dendritic solidification in an Al-10 wt.% Cu alloy, *Acta Mater.*, Vol 57, 2009, p 2300-2310

[5] S. Ilie, H. Preßlinger, P. Reisinger, M. Mayr, and K. Etzelsdorfer, Results of Research into the Segregation Behaviour of Manganese, Silicon and Chromium in Continuous Casting, *Steel Res. Int.*, Vol 78 (No 4), 2007, p 327-332

[6] M. Mayr, Metallic Embedding of Samples for EPMA, Internal working instruction, voestalpine Stahl GmbH, Linz, 2003

[7] M. Schaffer, J. Wagner, B. Schaffer, M. Schmied, and H. Mulders, Automated three-dimensional X-ray analysis using a dual-beam FIB, *Ultramicroscopy*, Vol 107, 2007, p 587-597

[8] R. C. Gonzalez, R. E. Woods, and S. L. Eddins, Digital Image Processing Using MATLAB, Prentice Hall, 2004, ISBN 978-0-13008-519-1

[9] W. Burger, and M. J. Burge, Digitale Bildverarbeitung, Springer, 2006, ISBN 978-3-540-30940-6

[10] J. Domitner, A. Kharicha, M. Grasser, and A. Ludwig, Reconstruction of Three-Dimensional Dendritic Structures based on the Investigation of Microsegregation Patterns, *Steel Res. Int.*, 2010, in press

[11] G. R. Speich, and R. M. Fisher, Recrystallization of a Rapidly Heated 3¼% Silicon Steel, *Sem. Proc.: Recrystallization, Grain Growth and Textures*, Metals Park, OH: ASM, 1966, p 563-598

[12] J. W. Cahn, The Significance of Average Mean Curvature and Its Determination By Quantitative Metallography, *Trans. AIME*, Vol 239, 1967, p 610-616

[13] B. B. Rath, The overall kinetics of isothermal transformations, *Conf. Proc.: Solid-Solid Phase Transformations*, Warrendale, PA: TMS-AIME, 1982, p 1097-1103

[14] L. Ratke, and A. Genau, Evolution of specific surface area with solid fraction during solidification, *Acta Mater.*, Vol 58, 2010, p 4207-4211